

(2) (M)

AD-A208 670

OFFICE OF NAVAL RESEARCH

GRANT N00014-88-K-0493

R & T Code 412m008

Technical Report No. 6

**OBSERVATION OF 'MAGIC NUMBERS'  
IN THE POPULATION DISTRIBUTION OF THE  
(NH<sub>3</sub>)<sub>n</sub>-1NH<sub>2</sub><sup>+</sup> and (NH<sub>3</sub>)<sub>n</sub>H<sub>2</sub><sup>+</sup> CLUSTER IONS:  
IMPLICATIONS FOR CLUSTER ION STRUCTURE**

by

William R. Peifer, M. Todd Coolbaugh and James F. Garvey\*

SDTIC  
ELECTE  
JUN 06 1989  
D CS D

Prepared for Publication  
in  
The Journal of Chemical Physics

Acheson Hall  
Department of Chemistry  
University at Buffalo  
The State University of New York at Buffalo  
Buffalo, NY  
14214

Reproduction in whole or in part is permitted for any purpose of the United States Government

This document has been approved for public release and sale; its distribution is unlimited

89 6 06 002  
05 157

## REPORT DOCUMENTATION PAGE

1a. REPORT SECURITY CLASSIFICATION <b>Unclassified</b>			1b. RESTRICTIVE MARKINGS			
2a. SECURITY CLASSIFICATION AUTHORITY			3. DISTRIBUTION / AVAILABILITY OF REPORT Approved for public release; distribution unlimited			
2b. DECLASSIFICATION / DOWNGRADING SCHEDULE			4. PERFORMING ORGANIZATION REPORT NUMBER(S) <b>Technical Report #6</b>			
6a. NAME OF PERFORMING ORGANIZATION <b>SUNY/Buffalo</b>			6b. OFFICE SYMBOL (if applicable)		7a. NAME OF MONITORING ORGANIZATION <b>Office of Naval Research</b>	
6c. ADDRESS (City, State, and ZIP Code) <b>Dept. of Chemistry, Acheson Hall, SUNY/Buffalo, Buffalo, NY 14214</b>			7b. ADDRESS (City, State, and ZIP Code) <b>Chemistry Program 800 N. Quincy St., Arlington, VA 22217</b>			
8a. NAME OF FUNDING / SPONSORING ORGANIZATION <b>Office of Naval Research</b>		8b. OFFICE SYMBOL (if applicable)		9. PROCUREMENT INSTRUMENT IDENTIFICATION NUMBER <b>#N00014-88-K-0483</b>		
8c. ADDRESS (City, State, and ZIP Code) <b>Chemistry Program, 800 N. Quincy St., Arlington, VA 22217</b>			10. SOURCE OF FUNDING NUMBERS			
			PROGRAM ELEMENT NO	PROJECT NO	TASK NO	WORK UNIT ACCESSION NO
11. TITLE (Include Security Classification) <b>OBSERVATION OF "MAGIC NUMBERS" IN THE POPULATION DISTRIBUTIONS OF THE (NH<sub>3</sub>)<sub>n-1</sub>NH<sub>2</sub><sup>+</sup> AND (NH<sub>3</sub>)<sub>n</sub>H<sub>2</sub><sup>+</sup> CLUSTER IONS: IMPLICATIONS FOR CLUSTER ION STRUCTURE</b>						
12. PERSONAL AUTHOR(S) <b>William R. Peifer, M. Todd Coolbaugh, and James F. Garvey</b>						
13a. TYPE OF REPORT <b>Technical</b>		13b. TIME COVERED FROM _____ TO _____		14. DATE OF REPORT (Year, Month, Day)		15. PAGE COUNT
16. SUPPLEMENTARY NOTATION <b>Journal of Chemical Physics</b>						
17. COSATI CODES			18. SUBJECT TERMS (Continue on reverse if necessary and identify by block number)			
FIELD	GROUP	SUB-GROUP	<b>Ammonia, hydrogen, clusters, (magic)</b>			
19. ABSTRACT (Continue on reverse if necessary and identify by block number)						
<p>We present the relative yields of the cluster ions, (NH<sub>3</sub>)<sub>n-1</sub>NH<sub>2</sub><sup>+</sup> and (NH<sub>3</sub>)<sub>n</sub>H<sub>2</sub><sup>+</sup>, produced by electron impact ionization of a supersonic molecular beam of neutral ammonia clusters, as functions of cluster ion size, neutral beam stagnation temperature, and electron impact energy. Our observation of a magic number at n = 7 in the distribution of (NH<sub>3</sub>)<sub>n-1</sub>NH<sub>2</sub><sup>+</sup> cluster ions is interpreted in terms of an intracuster bimolecular association reaction between a nascent NH<sub>2</sub><sup>+</sup> daughter ion and an adjacent NH<sub>3</sub> solvent molecule, giving rise to a protonated hydrazine product ion. Our observation of magic numbers at n = 5 and n = 8 in the (NH<sub>3</sub>)<sub>n</sub>H<sub>2</sub><sup>+</sup> cluster ion distribution is consistent with the production of the N<sub>2</sub>H<sub>8</sub><sup>+</sup> Rydberg radical cation via an intracuster ion-molecule reaction. The dependence of the yields of these solvated Rydberg radical cations on the stagnation temperature of the neutral molecular beam supports the notion that extensive solvation destabilizes these cluster ions.</p>						
20. DISTRIBUTION / AVAILABILITY OF ABSTRACT <input checked="" type="checkbox"/> UNCLASSIFIED/UNLIMITED <input type="checkbox"/> SAME AS RPT <input type="checkbox"/> DTIC USERS				21. ABSTRACT SECURITY CLASSIFICATION <b>Unclassified</b>		
22a. NAME OF RESPONSIBLE INDIVIDUAL <b>Dr. David L. Nelson</b>			22b. TELEPHONE (Include Area Code) <b>(202) 696-4410</b>		22c. OFFICE SYMBOL	

submitted to J.C.P. 6/3/89

Observation of "Magic Numbers" in the Population Distributions of the  $(\text{NH}_3)_{n-1}\text{NH}_2^+$  and  $(\text{NH}_3)_n\text{H}_2^+$  Cluster Ions: Implications for Cluster Ion Structures

William R. Peifer, M. Todd Coolbaugh, and James F. Garvey\*  
Department of Chemistry  
State University of New York at Buffalo  
Buffalo, New York 14214

Abstract

We have measured the relative yields of the cluster ions,  $(\text{NH}_3)_{n-1}\text{NH}_2^+$  and  $(\text{NH}_3)_n\text{H}_2^+$ , produced by electron impact ionization of a supersonic molecular beam of neutral ammonia clusters, as functions of cluster ion size, neutral beam stagnation temperature, and electron impact energy. Our observation of a magic number at  $n=7$  in the distribution of  $(\text{NH}_3)_{n-1}\text{NH}_2^+$  cluster ions is interpreted in terms of an intracuster bimolecular association reaction between a nascent  $\text{NH}_2^+$  daughter ion and an adjacent  $\text{NH}_3$  solvent molecule, giving rise to a protonated hydrazine product ion. Our observation of magic numbers at  $n=5$  and  $n=8$  in the  $(\text{NH}_3)_n\text{H}_2^+$  cluster ion distribution is consistent with the production of the  $\text{N}_2\text{He}^+$  Rydberg radical cation via an intracuster ion-molecule reaction. The dependence of the yields of these solvated Rydberg radical cations on the stagnation temperature of the neutral molecular beam supports the notion that extensive solvation destabilizes these cluster ions. Our experimental results are consistent with recent theoretical predictions concerning the structure and stability of the  $\text{N}_2\text{He}^+$  ion.

Accession For	
NTIS CRA&I	<input checked="" type="checkbox"/>
DTIC TAB	<input type="checkbox"/>
Unannounced	<input type="checkbox"/>
Justification	
By	
Distribution	
Availability Codes	
Dist	Availability Codes
A-1	

## Introduction

Nucleation processes and cluster formation are of fundamental significance in our understanding of condensed matter physics.<sup>1-3</sup> These processes play a central role in such diverse physical phenomena as crystal growth in solution and at interfaces, soot formation in flames, aerosol formation in the upper atmosphere, and particulate formation in the interstellar environment. Insights drawn from experiment and theory allow us to answer, at least in a qualitative way, questions regarding the stability of clusters as a function of size and structure, and the relative importance of each of the various intermolecular forces within these clusters. Some simple, intuitively appealing theoretical models have recently been brought to bear upon the problem of atomic cluster stability and its dependence on cluster size. Because of the fruitful marriage of mass spectrometry and various techniques for the generation of cluster beams, it has been possible in some cases to experimentally verify theoretical predictions of these models.

The simplest of models is based on geometric considerations,<sup>4</sup> and is applicable to clusters in which the pair potential (i.e., the interaction between the  $i$ -th and  $j$ -th particles within the cluster) is weak and centrosymmetric, and the total Hamiltonian is closely approximated by the sum over  $i$  and  $j$  of the spatial integrals of the pair potential. Stability is enhanced by maximizing contact between particles (via solid packing) while minimizing surface area; hence, the growing clusters attempt to assume a spherical, or nearly spherical, geometry. Structures predicted to have enhanced stability are the solid Mackay icosahedra containing  $N$  particles:

$$\begin{aligned}
 N_i &= (1/3)(10i^3 - 15i^2 + 11i - 3), \\
 &= 1, 13, 55, 147, 309, 561, \dots \quad (1)
 \end{aligned}$$

where the index,  $i$ , can take on any positive, non-zero integer value. The predominance of these icosahedral structures in the growth of rare gas neutral clusters has been demonstrated by dynamic computer simulations and gas-phase electron diffraction spectroscopy,<sup>5</sup> as well as cluster beam photoionization mass spectroscopy.<sup>6</sup>

A more sophisticated model, the so-called jellium model,<sup>7</sup> considers clusters not as a collection of neutral particles held by weak dispersive interactions, but as an ensemble of particles that can be separated into positively charged cores and valence electrons. The cores are assumed to be smeared out into a structureless "jelly" of positive charge, permeated by a uniform cloud of itinerant electrons. Potential functions are included in the Hamiltonian to account for core-core, core-electron, and electron-electron interactions. Since the cores within a cluster are assumed to be separated by distances which are large in comparison to their sizes, the core-core interactions can be treated with a simple Coulomb potential. The core-electron potential must contain both an attractive term (interaction of valence electrons with the positive core) and a repulsive term (interaction of valence electrons with core electrons). The net result is that the core-electron interactions are weak. The electron-electron interactions are treated within the context of the local density approximation;<sup>8</sup> that is, the interaction potential at  $r$  is a function of the local charge density at  $r$ . The potential must account for electron exchange and correlation. These terms, as well as the term describing electron kinetic energy, can be described parametrically as functions of  $r_s$ , the radius of the spherical volume element swept out by a single gaseous electron:

$$(4/3)\pi(r_s a_0)^3 = v/N(e) \quad (2)$$

where  $a_0$  is the Bohr radius,  $v$  is the volume of the electron cloud, and  $N(e)$  is the total number of electrons in the cloud. The kinetic, exchange, and correlation energies per electron can then be expressed in terms of  $r_s$ .<sup>9</sup> The total Hamiltonian for the system can then be written as the sum over all cores of the kinetic and Coulombic energies of the cores, plus the sum over all electrons of the kinetic, exchange, and correlation energies of the electrons. The energy eigenstates of this Hamiltonian are discrete and resemble those of a hydrogenic atom; however, the fact that the resultant cluster potential is not Coulombic in form allows the quantum number corresponding to orbital angular momentum to assume values greater than or equal to the principal quantum number. The spherical symmetry of the resultant potential leads to degeneracies in these eigenstates, resulting in electronic shell structure. *Enhanced cluster stability is a consequence of the closing of electronic shells and depends therefore on the total number of valence electrons, rather than upon core number or structure.* This model predicts shell closings for  $N(e) = 2, 8, 18, 20, 34, 40$ , and so on. This prediction has been experimentally verified by the observation of "magic numbers", or enhanced populations at certain values of  $N(e)$ , in the abundance spectra of neutral Na and K clusters,<sup>10</sup> positive cluster ions of noble metals,<sup>11,12</sup> and negative cluster ions.<sup>13,14</sup>

While the approximations of the jellium model are particularly valid for modeling metal clusters, they tend to break down for the treatment of clusters of molecules and non-metallic atoms. Charge distributions in clusters held together by covalent or hydrogen bonds are not expected to be uniform, and the angular dependence of the core-core potential (viz., the constraints imposed by orbital symmetry) is expected to give rise to preferential cluster geometries. For instance, carbon clusters seem to grow as hollow polyhedra

constructed of fused alicyclic rings. Enhanced stability is imparted when ring strain is minimized; hence, one would expect polyhedra constructed of fused five- and six-membered rings to be especially stable. This contention is experimentally corroborated by the observation of a magic number in the carbon cluster ion distribution at  $N=60$ , attributed to the hollow dodecahedral structure, "buckminsterfullerene".<sup>15</sup> Likewise, cluster ions which may form intracluster hydrogen bonds are found to display magic numbers, as evidenced by the particularly stable cluster ions:  $(\text{NH}_3)_4\text{NH}_4^+$  (thought to have tetrahedral symmetry<sup>16</sup>); and the species,  $(\text{H}_2\text{O})_{20}\text{H}_3\text{O}^+$ ,  $(\text{H}_2\text{O})_{20}(\text{NH}_3)_m\text{H}^+$  ( $m=1$  to  $6$ ), and  $(\text{H}_2\text{O})_{27}\text{NH}_4^+$  (thought to have ion clathrate structures<sup>17-19</sup>). Although fully elaborated *ab initio* theories of the structure and stability of large molecular clusters remain just beyond the frontiers of computational tractability, it is certainly clear that we can gain qualitative insights on molecular cluster structure and stability from a systematic search for magic numbers in cluster abundance spectra. We report in this Article our results for a study of product ions resulting from electron impact ionization of  $\text{NH}_3$  clusters, and we rationalize these results in terms of some intuitive structural models.

### Experimental Section

The experimental apparatus has been described in detail elsewhere<sup>20</sup> and is illustrated schematically in Figure 1. Briefly, the apparatus consists of a differentially pumped Campargue continuous molecular beam source<sup>21</sup> coupled to an Extrel C-50 quadrupole mass spectrometer. Anhydrous  $\text{NH}_3$  (Linde, 99.99%) is introduced into the stagnation volume of the apparatus in order to maintain a stagnation pressure of 1 atm. Neutral clusters form in the free-jet expansion created as the high-pressure gas expands adiabatically through a 250

$\mu\text{m}$  diameter nozzle into the source chamber. The neutral cluster population distribution can be regulated to a great extent by changing the nozzle temperature. In these experiments, the nozzle was typically maintained (within  $\pm 0.1$  K) at temperatures within the range of 253 to 313 K by a recirculating chiller. Pressure in the source chamber is maintained at about 50  $\mu\text{Torr}$  during operation of the cluster beam by a 1000  $\text{m}^3/\text{hr}$  roots blower. The cluster beam passes from the source chamber, through a 0.5 mm diameter skimmer (about 30 nozzle diameters downstream from the start of the expansion), and into a collimation chamber. This chamber is pumped by a 360 l/sec turbopump and is maintained at  $10^{-5}$  Torr during beam operation. The beam passes out of the collimation chamber through a second 0.5 mm diameter skimmer and into the mass spectrometer chamber. This chamber is also pumped by a 360 l/sec turbopump and is maintained at  $5 \times 10^{-7}$  Torr during beam operation.

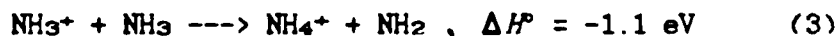
The cluster beam enters the ion source and quadrupole mass filter in an axial configuration. The mass filter is typically operated at better than 0.3 amu mass resolution up to about 1200 amu,<sup>22</sup> although we can select the best compromise between resolution and sensitivity, depending on the demands of a particular experiment. Emission current in the source is maintained at 1 mA by current regulation at fixed electron energy. In these experiments, mass spectra were collected at various electron kinetic energies ranging from about 40 to 100 eV. Cluster ions and fragments formed in the ion source are filtered by the quadrupole and imaged onto an off-axis channeltron. The amplified signal from the channeltron is then averaged by a digital storage oscilloscope.

In order to assure the validity of the mass spectral data, we regularly calibrated the mass scale and the sensitivity of the quadrupole mass

spectrometer. In the range below 500 amu, we calibrated the instrument against the mass spectrum of perfluorotributylamine; beyond 500 amu, we used an argon cluster beam as a calibration standard.

## Results and Discussion

**Ion Intensities.** The high-resolution electron impact mass spectrum of  $\text{NH}_3$  clusters can be described as an exponentially decaying progression of quartets. In the limit of low electron kinetic energy, this exponential decay is primarily a reflection of the population distribution in the neutral beam. A portion of the mass spectrum, which is illustrated in Figure 2, shows the quartet corresponding to cluster ions containing 25 nitrogen atoms. The peak labeled P represents the unreacted parent peak,<sup>23</sup> while the peak labeled 1 represents the solvated product of the intracuster ion-molecule reaction corresponding to the bimolecular analog:<sup>24</sup>



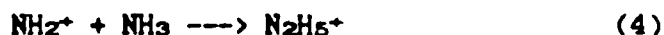
Peak a corresponds to cluster ions with the empirical formula,  $(\text{NH}_3)_{24}\text{NH}_2^+$ . The *nascent* ions can be thought of as solvated daughter ions, resulting from unimolecular fragmentation of the solvated  $\text{NH}_3^+$  parent. One might suspect this daughter ion to undergo subsequent intracuster ion-molecule reactions on the timescale of the experiment (*vide infra*). Peak a' corresponds to a cluster ion with the empirical formula,  $(\text{NH}_3)_{25}\text{H}_2^+$ . It has been suggested that this cluster ion represents the solvated product of an unusual intracuster ion-molecule reaction having no known gas-phase bimolecular analog.<sup>25</sup> Although a small part of the intensity of this peak may be attributed to the presence of  $\text{H}_2\text{O}$  in the clusters<sup>26</sup> (due to water contamination in the stagnation chamber), results from the experiments herein, as well as results from previous experiments in our laboratory on doubly

charged  $\text{NH}_3$  clusters,<sup>20</sup> support the identity of this cluster ion as an unusual nitrogen-containing species formed via an intracuster ion-molecule reaction.

A mechanism accounting for the mass spectral features described above is shown schematically in Figure 3. We now wish to consider the relative abundance of these cluster ions as a function of cluster size. Castleman and co-workers<sup>18</sup> have examined the population distribution of the cluster ions,  $(\text{NH}_3)_{n-1}\text{NH}_4^+$ , and have observed a "magic number" at  $n=5$ , corresponding to the particularly stable tetrahedral cluster ion,  $(\text{NH}_3)_4\text{NH}_4^+$ . We discuss below the appearance of "magic numbers" in the population distributions of the ions,  $(\text{NH}_3)_{n-1}\text{NH}_2^+$  and  $(\text{NH}_3)_n\text{H}_2^+$ , and interpret these findings in terms of structural models.

**The  $(\text{NH}_3)_{n-1}\text{NH}_2^+$  Cluster Ions.** A plot of the relative intensities of the  $(\text{NH}_3)_{n-1}\text{NH}_2^+$  ions as a function of cluster size  $n$  is shown in Figure 4. A magic number, corresponding to enhancement in the ion signal, is observed for the cluster ion of size  $n=7$ . This enhancement at  $n=7$ , relative to ion yield at  $n \geq 11$ , is independent of electron impact energy, although absolute ion yields are observed to increase as a function of electron impact energy. As shown in Figure 5, this relative enhancement appears to increase somewhat as the nozzle temperature is increased. This is presumably due to a more rapid exponential decay of the neutral cluster beam population distribution (i.e., a smaller number of larger clusters) under conditions of higher stagnation temperatures.

We can account for the observed size dependence of the  $(\text{NH}_3)_{n-1}\text{NH}_2^+$  cluster ion yield if we assume that an associative ion-molecule reaction occurs between the nascent  $\text{NH}_2^+$  ion and an adjacent  $\text{NH}_3$  solvent molecule within the cluster:



From available thermochemical data,<sup>27,28</sup> we estimate that this reaction is exothermic by 4.52 eV. A similar (albeit endothermic) bimolecular reaction is known to occur between  $\text{NH}_3^+$  and  $\text{NH}_3$ :



at a rate which is about 0.1% of gas-kinetic.<sup>29,30</sup> We expect the barrier for reaction (4) to be smaller than that for reaction (5) for the following reasons. First, within the context of the Hammond postulate,<sup>31</sup> the barrier to reaction (4) is expected to occur earlier along the reaction coordinate, the potential surface is expected to be more attractive, and the transition state is expected to more closely resemble the reactants. Second, the activation energy for reaction (4) is expected to be lower than that of reaction (5), since the transition state for (5) must contain at least one highly extended N-H bond (correlating with eventual loss of the product H atom). By analogy with other associative bimolecular reactions, we would expect the activation energy for reaction (4) to be small, if not negligible, and determined to a great extent by the dipole-dipole interaction.<sup>32</sup> Third, the symmetry contribution to the barrier for (5) is probably larger than that for (4), due to the N-H bond distortion (and subsequent reduction in symmetry number) in the transition state for (5). We might therefore expect, based on differences in activation energies and Arrhenius A factors, that the associative reaction (4) will proceed at a rate significantly greater than 0.1% of the gas-kinetic rate.

While the "naked" (unclustered) product of the highly exothermic associative reaction (4) would have sufficient internal energy to undergo subsequent N-H bond cleavage, it would certainly be stabilized through solvation by additional  $\text{NH}_3$  molecules. In fact, if we hydrogen-bond five  $\text{NH}_3$  solvent molecules to the five H atoms of the  $\text{N}_2\text{H}_5^+$  product ion, we end up with

an ion having a completed solvation shell with the empirical formula,  $(\text{NH}_3)_n\text{NH}_4^+$ , as illustrated in Figure 6. This cluster ion has a total of seven N atoms and accounts for our observation of a magic number,  $n=7$ .

**The  $(\text{NH}_3)_n\text{NH}_4^+$  Cluster Ions.** A plot of the intensities of the  $(\text{NH}_3)_n\text{NH}_4^+$  ions as a function of cluster size  $n$  is shown in Figure 7. Two magic numbers are observed in the cluster ion population distribution, corresponding to enhanced stability of the  $n=5$  and  $n=8$  cluster ions. The relative enhancements at  $n=5$  and  $n=8$  (compared to cluster ions of size  $n \geq 11$ ) are independent of electron impact energy, although absolute ion yields are again observed to increase at higher energy. These enhancements appear to increase dramatically as the stagnation temperature is increased from 253 to 273 K, as shown in Figure 8. The increase in relative enhancement as a function of increasing stagnation temperature is more gradual at temperatures above 273 K. This temperature dependence will be discussed in greater detail below.

One might argue that we are not really observing cluster ions of the form  $(\text{NH}_3)_n\text{NH}_4^+$ , but rather the isobaric species  $(\text{H}_2\text{O})(\text{NH}_3)_{n-2}\text{NH}_4^+$ .<sup>28</sup> Such heteroclusters can be thought of as solvated  $\text{NH}_4^+$  ions in which one of the  $\text{NH}_3$  solvent molecules has been replaced by an  $\text{H}_2\text{O}$  molecule. These heteroclusters would be expected to have structures analogous to those of the  $(\text{NH}_3)_{n-1}\text{NH}_4^+$  cluster ions, and would therefore display magic numbers in the population distribution at  $n=5$  (packed tetrahedron)<sup>18</sup> and  $n=9$  (packed dodecahedron),<sup>33</sup> as observed for solvated  $\text{NH}_4^+$  cluster ions. However, we do not observe magic numbers at these  $n$  values, but rather at  $n=5$  and  $n=8$ . Therefore, we believe that what we are observing is the series of cluster ions,  $(\text{NH}_3)_n\text{NH}_4^+$ , and not isobaric interferences from  $\text{H}_2\text{O}$ -containing heteroclusters.

Such a molecular formula implies some interesting structural possibilities. Garvey and Bernstein originally suggested<sup>25</sup> that these cluster

ions might arise from intracluster ion-molecule reactions which give rise to a solvated  $\text{NH}_5^+$ , a hypervalent species with trigonal bipyramidal symmetry. Such a structure is consistent with the results of *ab initio* calculations,<sup>34</sup> although a minimum in the hypersurface is achieved only if the system is "Rydbergized".<sup>35</sup> We might expect that an  $\text{NH}_5^+$  ion solvated by five  $\text{NH}_3$  solvent molecules would show enhanced stability, by analogy with  $(\text{NH}_3)_4\text{NH}_4^+$ , and that the population distribution of  $(\text{NH}_3)_{n-1}\text{NH}_5^+$  cluster ions would therefore display a magic number at  $n=6$ . However, we do not observe a magic number at  $n=6$ , and we cannot account for our observed magic numbers on the basis of solvation of a trigonal bipyramidal species. Recent *ab initio* calculations at the unrestricted Hartree-Fock level<sup>36</sup> suggest that the unsolvated ion is actually a Rydberg radical ion,  $\text{N}_2\text{H}_6^+$ , whose predicted structure is shown in Figure 9. One might expect that an  $\text{N}_2\text{H}_6^+$  ion solvated (via hydrogen bonding) at each of its six available H sites would display enhanced stability with respect to species of different degrees of solvation. The population distribution of  $(\text{NH}_3)_{n-2}(\text{N}_2\text{H}_6)^+$  cluster ions would therefore show a magic number at  $n=8$ ; this is precisely what we observe experimentally. Our observation of magic numbers at  $n=5$  and  $n=8$  can be accounted for on the basis of the two structures shown in Figure 10. Apparently, enhanced stability is imparted even when only one of the ion's nitrogen centers is completely solvated; that is, when the solvation shell surrounding the  $\text{N}_2\text{H}_6^+$  ion is only half-full.

Kassab *et al.* suggest,<sup>36</sup> by analogy with the  $\text{NH}_4$  Rydberg radical,<sup>37</sup> that extensive solvation of  $\text{N}_2\text{H}_6^+$  may actually *destabilize* the radical cation cluster. Hence, one might expect to observe  $(\text{NH}_3)_{n-2}\text{N}_2\text{H}_6^+$  cluster ions only for small to moderate values of  $n$ . If one were to prepare these cluster ions by electron impact ionization of a molecular beam of neutral clusters of  $\text{NH}_3$

(as we have done), one might then expect to observe *greater* yields of  $(\text{NH}_3)_{n-2}\text{N}_2\text{He}^+$  when the neutral beam has an enriched population of *smaller* clusters. One way to attain such an enrichment is to operate the molecular beam expansion at elevated stagnation temperatures. In fact, we *do* observe an increase in the yields of these cluster ions as the stagnation temperature is increased, as shown in Figure 8. This observation represents experimental confirmation of the theoretical predictions of Kassab *et al.*<sup>36</sup>

### Conclusions

We have reported previously unobserved magic numbers in the population distributions of the cluster ions,  $(\text{NH}_3)_{n-1}\text{NH}_2^+$  and  $(\text{NH}_3)_n\text{H}_2^+$ , produced via electron impact ionization of a supersonic molecular beam of neutral  $(\text{NH}_3)_{n+1}$  clusters. We take the observation of a magic number of  $n=7$  in the solvated  $\text{NH}_2^+$  cluster ion distribution as evidence of an associative ion-molecule reaction between an  $\text{NH}_2^+$  daughter ion and an  $\text{NH}_3$  solvent molecule, giving rise to a protonated hydrazine molecule within an  $\text{NH}_3$  solvent shell. The magic numbers we observe in the  $(\text{NH}_3)_n\text{H}_2^+$  cluster ion population distribution can be explained in terms of a solvated  $\text{N}_2\text{He}^+$  Rydberg radical cation, and is inconsistent with production of solvated heterocluster ions of the form,  $(\text{H}_2\text{O})(\text{NH}_3)_{n-2}\text{NH}_4^+$ . Our results are consistent with the *ab initio* calculations of Kassab *et al.* on the structure and stability of the  $\text{N}_2\text{He}^+$  Rydberg radical cation. It is hoped that continuing experimental efforts, in our own laboratory as well as those of our colleagues, will stimulate the further elaboration and refinement of theoretical models dealing with the electronic structure of clusters and cluster ions.

*Acknowledgment* is made to the Office of Naval Research, and to the donors of the Petroleum Research Fund, administered by the American Chemical Society, for generous support of this research.

## REFERENCES

- (1) Hoare, M.R. *Adv. Chem. Phys.* 1979, 40, 49.
- (2) Märk, T.D.; Castleman, A.W., Jr. *Adv. At. Mol. Phys.* 1985, 20, 65.
- (3) Märk, T.D. *Int. J. Mass Spectrom. Ion Proc.* 1987, 79, 1.
- (4) Mackay, A.L. *Acta Cryst.* 1962, 15, 916.
- (5) Farges, J.; deFeraudv, M.F.; Raoult, B.; Torchet, G. *International Meeting on Small Particles and Inorganic Clusters*, Lyon-Villeurbanne, September 1976. *Journal de Physique Colloque C-2*, 1977, p. 47.
- (6) Schriver, K.E.; Hahn, M.Y.; Persson, J.L.; LaVilla, M.E.; Whetten, R.L. *J. Phys. Chem.* 1989, 93, 2869.
- (7) Cohen, M.L.; Chou, M.Y.; Knight, W.D.; de Heer, W.A. *J. Phys. Chem.* 1987, 91, 3141.
- (8) Kohn, W.; Sham, L.J. *Phys. Rev.* 1965, 140, A1333.
- (9) Kittel, C. *Introduction to Solid State Physics*, 6th ed.; Wiley: New York, 1986.
- (10) Knight, W.D.; Clemenger, K.; de Heer, W.A.; Saunders, W.A. *Solid State Commun.* 1985, 53, 445.
- (11) Katakuse, I.; Ichihara, I.; Fujita, Y.; Matsuo, T.; Sakurai, T.; Matsuda, H. *Int. J. Mass Spectrom. Ion Proc.* 1985, 67, 229.
- (12) Begemann, W.; Meiwes-Broer, K.H.; Lutz, H.O. *Z. Phys. D* 1986, 3, 109.
- (13) Hortig, G.; Müller, M. *Z. Phys.* 1969, 221, 119.
- (14) Joyes, P.; Sudraud, P. *Surf. Sci.* 1985, 156, 451.
- (15) Kroto, H.W.; Heath, J.R.; O'Brien, S.C.; Curl, R.F.; Smalley, R.E. *Nature* 1985, 318, 162.
- (16) Echt, O.; Morgan, S.; Dao, P.D.; Stanley, R.J.; Castleman, A.W., Jr. *Ber. Bunsenges. Phys. Chem.* 1984, 88, 217.

- (17) Kassner, J.L.; Hagen, D.E. *J. Chem. Phys.* 1978, 64, 1880.
- (18) Shinohara, H.; Nagashima, U.; Nishi, N. *Chem. Phys. Lett.* 1984, 111, 511.
- (19) Shinohara, H.; Nagashima, U.; Tanaka, H.; Nishi, N. *J. Chem. Phys.* 1985, 83, 4183.
- (20) Coolbaugh, M.T.; Peifer, W.R.; Garvey, J.F. *Chem. Phys. Lett.* 1989, 156, 19.
- (21) Campargue, R. *J. Phys. Chem.* 1984, 88, 4466.
- (22) Peifer, W.R.; Coolbaugh, M.T.; Garvey, J.F. *J. Phys. Chem.* 1989, 93, in press.
- (23) It is also possible that this "parent" peak represents, at least in part, the solvated product ion of Reaction (3); that is,  $(\text{NH}_3)_n\text{-2NH}_2\text{NH}_4^+$ . For larger clusters, reaction exothermicity may be carried away either by loss of the neutral  $\text{NH}_2$  product, or by evaporation of a surface  $\text{NH}_3$  solvent molecule. In the latter case, it is not possible to distinguish the unreacted parent cluster ion from the cluster ion which has undergone a bimolecular reaction. See, for example: Morgan, S.; Castleman, A.W., Jr. *J. Am. Chem. Soc.* 1987, 109, 2867.
- (24) Hogg, A.M.; Haynes, R.M.; Kebarle, P. *J. Am. Chem. Soc.* 1966, 88, 28.
- (25) Garvey, J.F.; Bernstein, R.B. *Chem. Phys. Lett.* 1988, 143, 13.
- (26) Shinohara, H.; Nishi, N. *Chem. Phys. Lett.* 1987, 141, 292.
- (27) Rosenstock, H.M.; Draxl, K.; Steiner, B.W.; Herron, J.T. *J. Phys. Chem. Ref. Data* 1977, 6, Suppl. Monograph 1.
- (28) Meot-Ner, M.; Nelsen, S.F.; Willi, M.R.; Frigo, T.B. *J. Am. Chem. Soc.* 1984, 106, 7384.

(29) Derwish, G.A.W.; Galli, A.; Giardini-Guidoni, A.; Volpi, G.G. *J. Chem. Phys.* 1963, 39, 1599.

(30) Melton, C.E. *J. Chem. Phys.* 1966, 45, 4414.

(31) Hammond, G.S. *J. Am. Chem. Soc.* 1955, 77, 334.

(32) Benson, S.W. *Thermochemical Kinetics*, 2nd ed.; Wiley: New York, 1976.

(33) In addition to the magic number,  $n=5$ , observed by Echt *et al.* for the  $(\text{NH}_3)_n\text{-1NH}_4^+$  clusters ions, we observe an additional magic number at  $n=9$ . We attribute this observation to the packing of four additional  $\text{NH}_3$  molecules along the four faces of the tetrahedron of  $(\text{NH}_3)_4\text{NH}_4^+$ , although we cannot rule out the possibility of an alternative packing configuration.

(34) Bugaets, O.P.; Zhogolev, D.A. *Chem. Phys. Lett.* 1977, 45, 462.

(35) Mulliken, R.S. *Accts. Chem. Res.* 1976, 9, 7.

(36) Kassab, E.; Fouquet, J.; Evleth, E.M. *Chem. Phys. Lett.* 1988, 153, 522.

(33) Kassab, E.; Evleth, E.M. *J. Am. Chem. Soc.* 1987, 109, 1653.

Figure 1. Schematic representation of the differentially pumped cluster beam apparatus and quadrupole mass spectrometer. The temperature of the nozzle in the stagnation region is regulated by a circulating chiller.

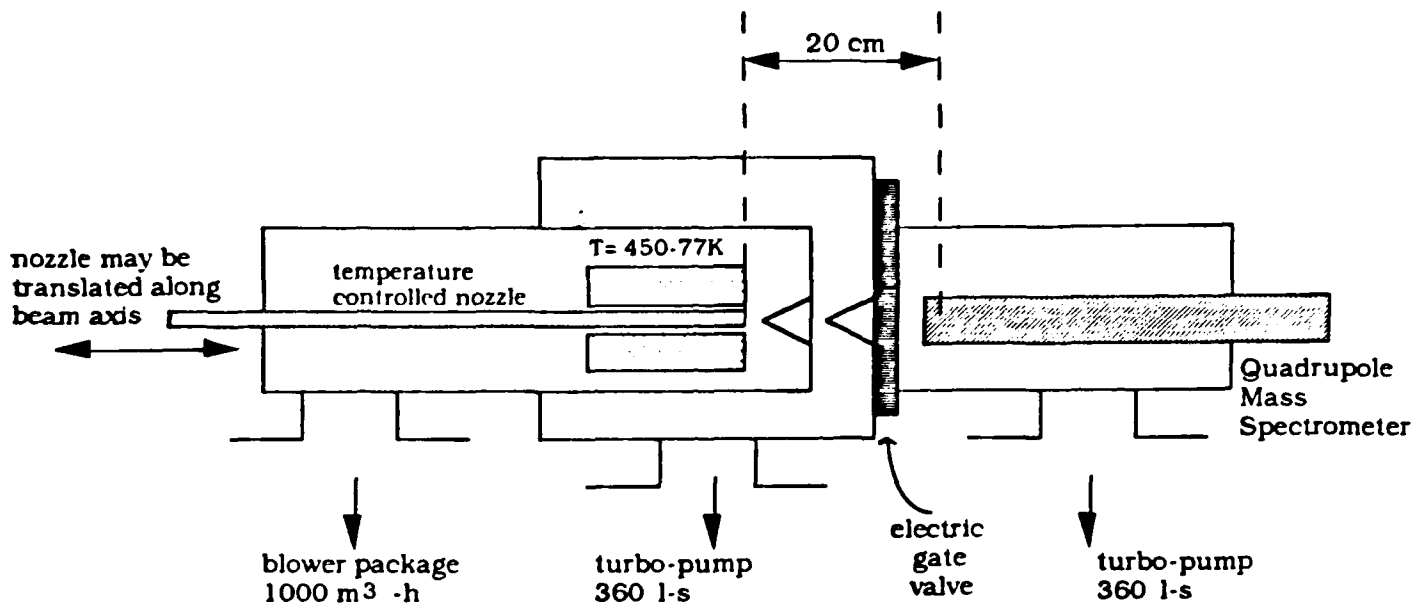


Figure 2. A representative portion of the 70 eV electron impact mass spectrum of the ammonia cluster beam. This portion of the spectrum corresponds to the four different cluster ion species containing 25 nitrogen atoms each. The abscissa is scaled according to the *nominal* masses for H and N of 1 and 14 amu, respectively.

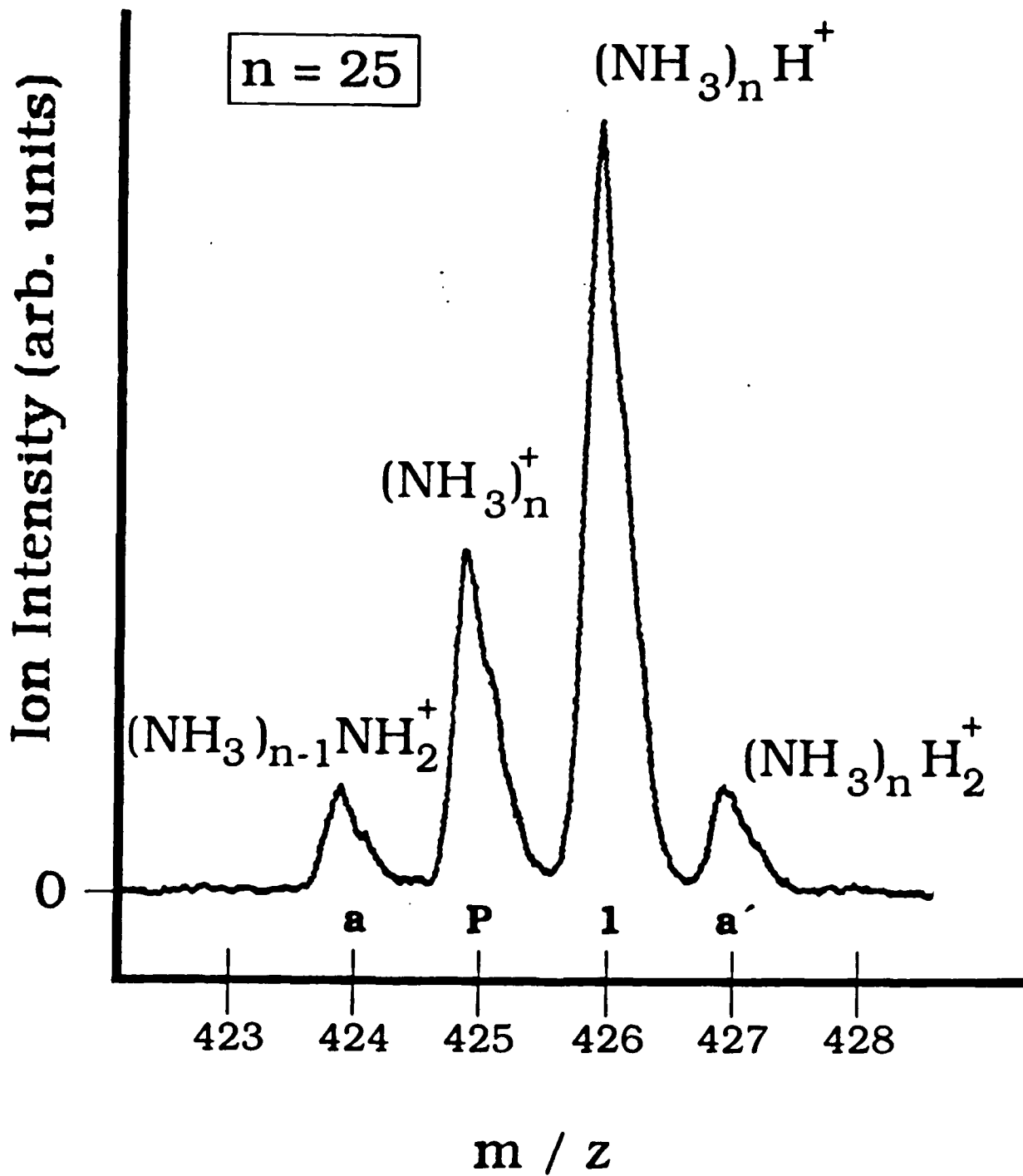


Figure 3. Schematic representation of the dynamical processes leading to formation of the various solvated product ions from the solvated parent. Differences in the shading of the indicated peaks is intended to indicate that the four peaks *do not* belong to the same family of n-mers. Peaks P and a are members of the family of (n+1)-mers, while peaks 1 and a' are members of the family of n-mers.

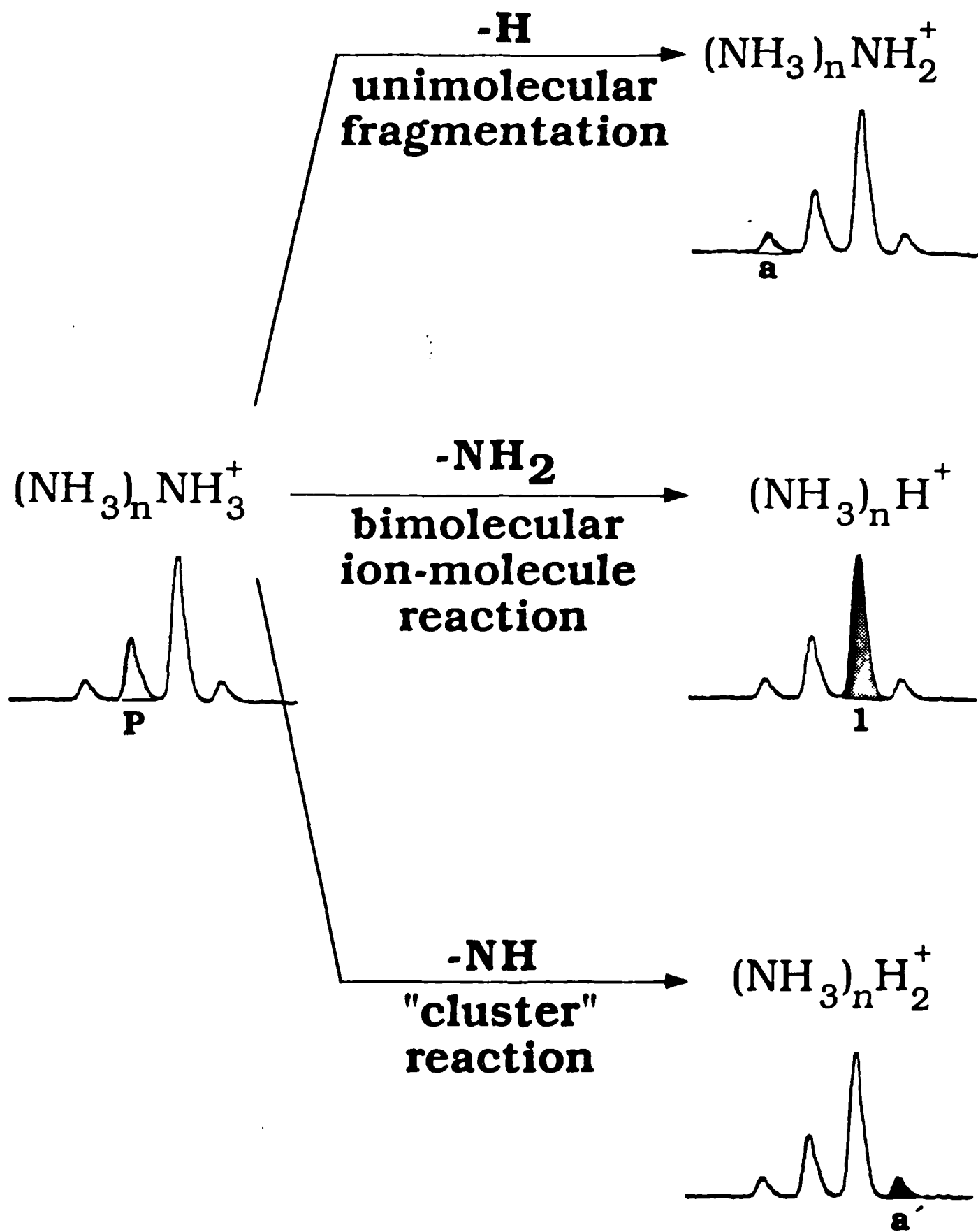


Figure 4. A plot of the intensities of the  $(\text{NH}_3)_{n-1}\text{NH}_2^+$  cluster ions versus cluster size,  $n$ . The stagnation temperature was held at 273 K during the collection of all mass spectra represented here. Note the magic number at  $n=7$ .

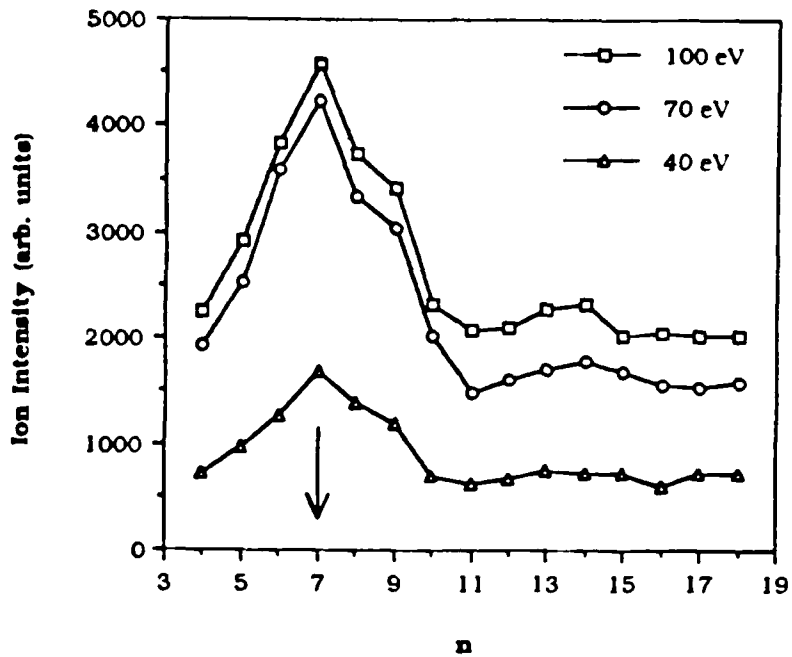


Figure 5. A plot of the intensities of the  $(\text{NH}_3)_{n-1}\text{NH}_2^+$  cluster ions versus stagnation temperature. The mass spectra represented here were all collected at an electron impact energy of 70 eV.

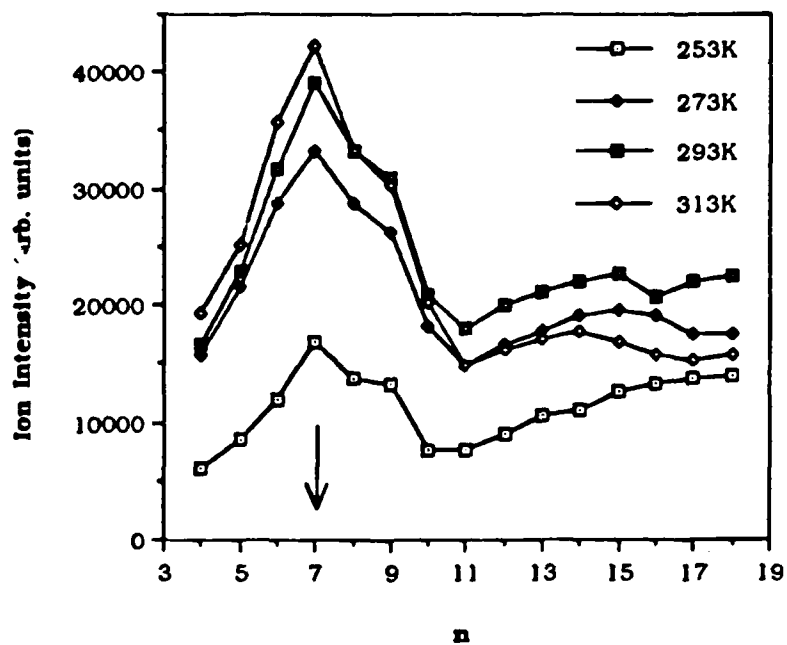


Figure 6. Proposed structure for the  $(\text{NH}_3)_n\text{NH}_2^+$  cluster ion. This species is the most prevalent of all cluster ions in the series,  $(\text{NH}_3)_{n-1}\text{NH}_2^+$ , and is believed to be a protonated hydrazine molecule surrounded by one complete solvation shell.

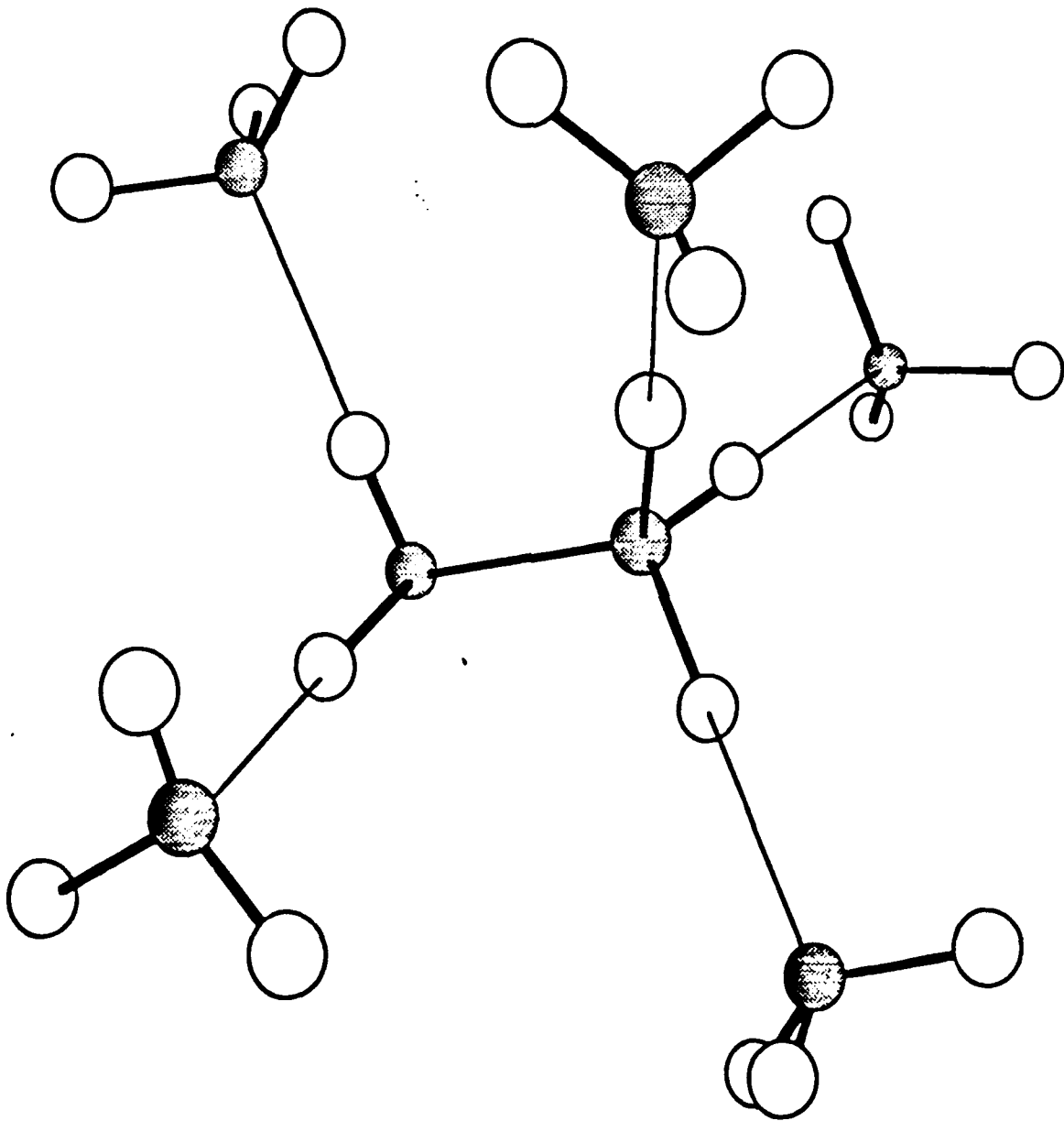


Figure 7. A plot of the intensities of the  $(\text{NH}_3)_n\text{H}_2^+$  cluster ions versus cluster size,  $n$ . The stagnation temperature was held at 273 K during the collection of all mass spectra represented here. Note the magic numbers at  $n=5$  and  $n=8$ .

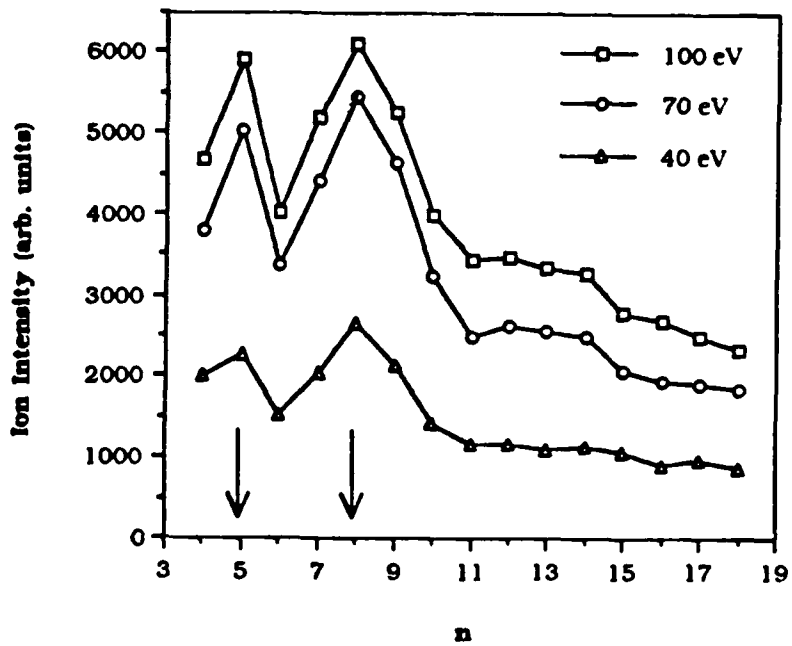


Figure 8. A plot of the intensities of the  $(\text{NH}_3)_n\text{H}_2^+$  cluster ions versus stagnation temperature. The mass spectra represented here were all collected at an electron impact energy of 70 eV. Note that the enhancement of the "magic" ion signals, relative to signals from the species larger than  $n=11$ , appears to increase dramatically as the stagnation temperature is increased from 253 K to 273 K. The degree of enhancement increases more gradually as the stagnation temperature is increased from 273 K to 313 K.

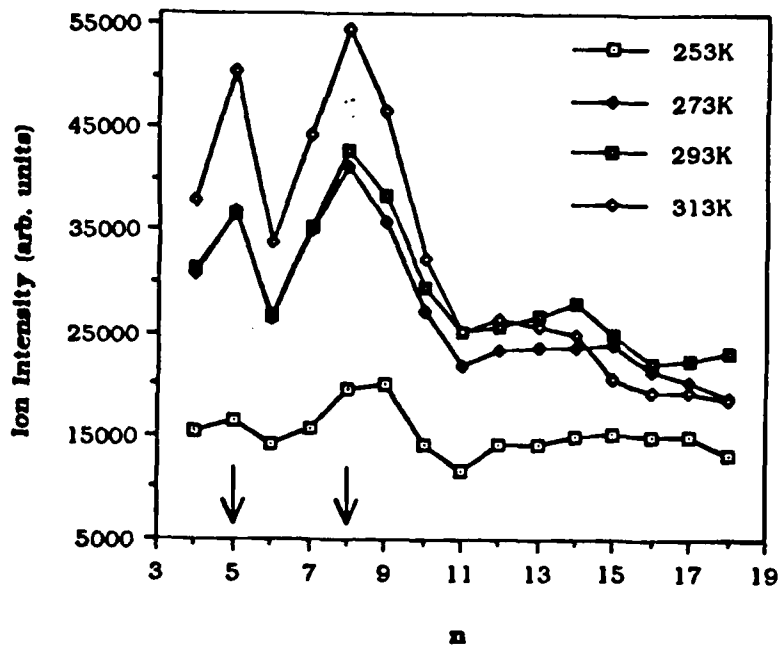


Figure 9. Proposed structure of the  $N_2He^+$  ion, after Kassab *et al.*<sup>36</sup> This species is predicted to be a Rydberg radical cation.

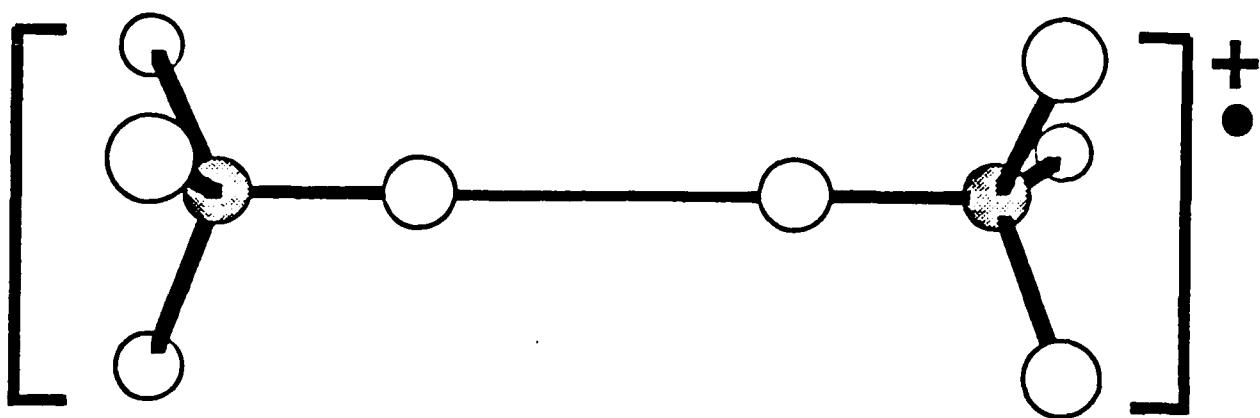
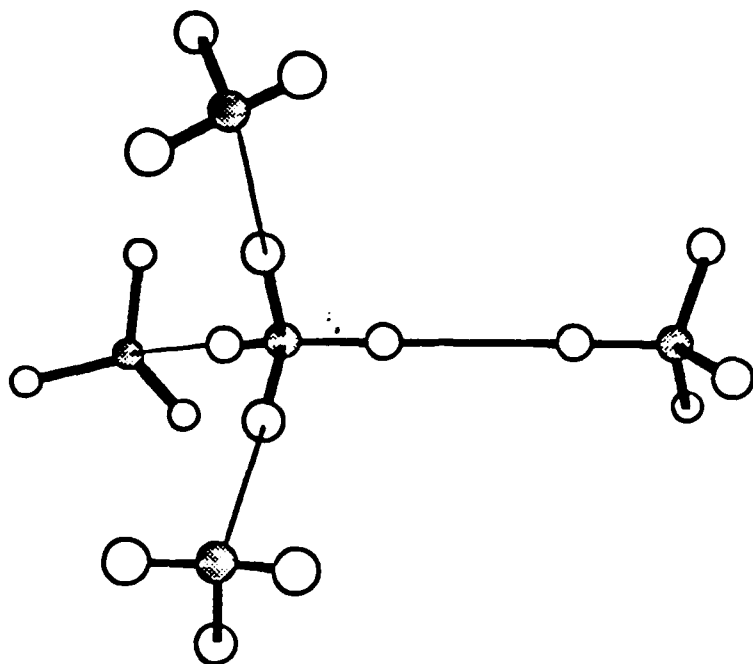


Figure 10. Proposed structures for: a) the  $(\text{NH}_3)_3\text{N}_2\text{H}_8^+$  cluster ion, and b) the  $(\text{NH}_3)_6\text{N}_2\text{H}_8^+$  cluster ion. These species represent the most stable solvated forms of the Rydberg radical cation,  $\text{N}_2\text{H}_8^+$ . Apparently, complete solvation of one end of this radical ion is sufficient to impart enhanced stability.

a)



b)

